Expected impact of the future SMOS and Aquarius Ocean surface salinity missions in the Mercator Ocean operational systems: new perspectives to monitor ocean circulation

Benoît Tranchant, Charles-Emmanuel Testut, Lionel Renault, Nicolas Ferry, Florence Birol, Pierre Brasseur

Expected impact of the future SMOS and Aquarius Ocean surface salinity missions in the Mercator Ocean operational systems: New perspectives to monitor ocean circulation

Benoît Tranchant [a,b,*], Charles-Emmanuel Testut [a], Lionel Renault [c], Nicolas Ferry [a], Florence Birol [c], Pierre Brasseur [d]

[a] *Mercator Océan, 8/10 rue Hermes, 31520 Ramonville-St-Agne, France*
[b] *CERFACS, 42 Av. Gaspard Coriolis, 31057 Toulouse Cedex 01, France*
[c] *LEGOS, 14 Av. Edouard Belin, 31400 Toulouse, France*
[d] *LEGI, B.P.53, 38041 Grenoble Cedex 9, France*

Abstract

Sea Surface Salinity (SSS) has never been observed from space. The SSS from planned satellite missions such as Soil Moisture and Ocean Salinity (SMOS) and Aquarius is a key to better understanding how ocean circulation is related to water cycle and how both these systems are changing through time.

The Observing System Simulation Experiments (OSSEs) presented in this paper has been carried out with an ocean forecasting system developed within the French oceanographic Mercator Ocean context. They consist in hindcast experiments assimilating an operational dataset (Sea Surface Temperature (SST), in-situ profiles of temperature and salinity and Sea Level Anomalies (SLA)) and various simulated SMOS and Aquarius Sea Surface Salinity (SSS) data. These experiments use an eddy permitting model (1/3°) covering the North Atlantic from 20°S to 70°N. The new generation of fully multivariate assimilation system referred to as SAM2v1 which is being developed from the SEEK (Singular Evolutive Extended Kalman) algorithm is used. This scheme is a Reduced Order Kalman Filter using a 3D multivariate modal decomposition of the forecast error covariance.

The OSSEs enabled us to show the positive impact of SSS assimilation on the Mercator Ocean operational forecasting system. These experiments particularly show the importance to specify appropriated observation errors and the impact of having and/or combining different observing system. Several conclusions can be highlighted such as the importance of the space/time scales consistency between the data products and our ocean prediction systems. This study has to be considered as an important step for assimilation of SSS measured from space. Further studies have to be conducted with other simulated data, other oceanic configurations and other improved assimilation schemes.

Keywords: Data assimilation; Sea Surface Salinity; OSSE

1. Introduction

Ocean salinity variability plays an active role and is a key indicator of the underlying processes that link the ocean circulation and hydrologic cycle (Lagerloef, 2002). Moreover, a better understanding of the interactions between hydrologic cycle, ocean circulation and global heat transport variations is essential for climate studies. Although salinity has little direct effect on the atmosphere, it is important in the formation of water masses and thus in the global ocean circulation. Salinity variability affects the circulation through density effects, in particular through horizontal pressure gradients (Cooper, 1988; Murtuggude and Busalacchi, 1998; Roemmich et al., 1994). Sea surface salinity largely controls the density of the surface layer, thereby affecting the intensity of North Atlantic deep convection

* Corresponding author.
E-mail address: benoit.tranchant@mercator-ocean.fr (B. Tranchant).

and playing an important role in the variability of the thermohaline circulation. In tropical oceans, salinity modulates vertical stratification, and can thus favour or inhibit vertical mixing (Godfrey and Lindstrom, 1989). Vertical stratification of salinity also impacts the surface layer momentum budget, by limiting mixed layer depth and increasing the response to wind forcing.

One can consider that the mean Sea Surface Salinity (SSS) is strongly related to the mean distribution of the Evaporation Minus Precipitation ($E-P$) budget. In addition, river runoff further affects the mean SSS distribution at regional scales: for example, off the Amazon and Congo rivers (Dessier and Donguy, 1994; Masson and Delecluse, 2001).

SSS records remain too sparse to document properly the SSS variability over most regions. However, recently, Delcroix et al. (2005) analysed an unprecedented compilation of SSS data (Volunteer Ship observations, TAO/TRITON and PIRATA arrays) collected in the three tropical oceans (30°N–30°S) for the period 1969–2003. After quality control procedures, Delcroix et al. (2005) have analysed the compilation of SSS data both as gridded fields (2° longitude, 1° latitude, 1 month) and as high-resolution records (0.02° latitude/longitude and one day). Delcroix et al. (2005) found that the SSS variability lies generally within 0.1–0.3 PSU in the studied regions, with however remarkable exceptions (the SSS standard deviation can reach locally 1.4 PSU). The largest values are found in the Indonesian Archipelago, in the South East of India, East of Panama, off the Amazon River mouth, under the Atlantic ITCZ (Inter Tropical Convergence Zone) and in the central Pacific. The SSS time scale is found to be generally less than three months in regions that have strong seasonal cycle, whereas it ranges within 4–8 months where the variability is mostly controlled by ENSO. The SSS meridional scale is about 2–3° in some regions (Atlantic Ocean, eastern half of the Pacific, etc.) and larger in others (western tropical Pacific warm pool, etc.). A SSS zonal correlation scale of about 15–20° longitude is found in the equatorial Pacific and in the South Pacific Convergence Zone (SPCZ) whereas it is about 4–7° longitude along 8–10°N in the Indian.

Thus, realistic simulation of SSS is essential for a successful representation of the ocean state. Unfortunately, important errors in the forcing fields and numerical ocean model shortcomings lead to significant errors in simulated salinity fields. A well-known deficiency of ocean models is their tendency to produce spurious drifts in SSS fields. For that reason, ocean modellers have adopted simplified forms of restoring to observations or climatology, or have developed new methods of modifying restoring boundary conditions as in Kamenkovich and Sarachik (2004). These methods of relaxation are mainly used to compensate the lack of reliable $E-P$ information. Indeed, a poor knowledge of the fresh water fluxes or the too large error in the $E-P$ budget is a real drawback. Thus, recent studies tend to improve these fresh water fluxes by combining numerical weather prediction (NWP) and satellite data sources (Yu et al., 2004). Another solution consists of estimating an ad hoc correction of the systematic biases of the forcing fluxes based on the relaxation term, and to constraint the model with the corrected forcing fluxes (Ferry and Reverdin, 2004; Vialard et al., 2002).

To compensate for errors due to the model physics or due to inaccurate initial conditions and errors in the specification of freshwater fluxes, one of the more powerful solutions consists of the assimilation of SSS data. There are still not enough studies that show the impact of SSS assimilation on ocean dynamic. For instance, Durand et al. (2002) and Durand et al. (2003) show the interest of assimilating SSS with a SEEK (Singular Extended Evolutive Kalman) filter in the tropical Pacific. Nevertheless, these studies were performed for ideal cases and/or for twin experiments.

Unlike other ocean parameters such as Sea Level Anomalies (SLA) or Sea Surface Temperature (SST) which are relatively well measured, there are few SSS measurements. In addition, SSS measurements are mainly confined to shipping lanes and the summer season. Nevertheless, over the last decade, it has been demonstrated that SSS can be measured from space and two missions will allow to map sea surface salinity in the near future (Font et al., 2000; Lagerloef and Delcroix, 2001): the SMOS (Soil Moisture and Ocean Salinity) mission and the proposed US/Argentinean Aquarius/SAC-D mission (e.g., Sen et al., 2006). These two missions should provide global ocean coverage measurements of SSS to the scientific community and should counterbalance the lack of sea surface salinity data.

The SMOS satellite should be launched in 2008 by the European Spatial Agency (ESA) to measure ocean surface salinity as well as moisture of continental surface from space and the US/Argentinean Aquarius/SAC-D satellite should also measure sea surface salinity from the year 2009.

A priori, the errors from satellite measurements should be larger than those of in-situ, but this drawback is compensated by the fact that the satellite data space-time coverage will make it possible to study large scale processes and their evolution over several years. Several levels of products will be available corresponding to various levels of data treatment. The main characteristics of these two missions are summarized in Table 1.

In order to make optimal use of future SSS data, the present paper addresses the impact of assimilating simulated SSS data in an Ocean General Circulation Model (OGCM) within an operational ocean forecasting context. Consequently, Observing System Simulation Experiments (OSSEs) have been performed

Table 1
SMOS and Aquarius mission main characteristics

Science satellite mission	SMOS	Aquarius
Scientific objectives	Observation of soil moisture and SSS	Observation of SSS
Measurements goals	– Accuracy of 0.5–1.5 PSU for a single observation – Accuracy of 0.1 PSU for a 10–30 days average and for an open ocean area of 200 km × 200 km	– Global monthly 150-kilometer resolution SSS maps with an accuracy of 0.2 PSU
Temporal and spatial resolutions	Global coverage every 3 days and ~45-kilometer resolution	Global coverage every 7 days and ~150-kilometer resolution

with simulated SMOS and Aquarius SSS data (level 2 products) and the new Mercator Ocean's (hereafter noted MO) multivariate assimilation system called SAM2v1 (Tranchant et al., 2005). Thus, the main objectives of this study are (i) to understand the most efficient way to assimilate SSS data in order to extract the best reliable information in the context of the MO forecasting system (ii) to evaluate the potential impact of two different observing systems, and (iii) to know the level of the observation error from which associated SSS data have a significant influence on the assimilation system SAM2v1.

This paper is organized as follows. Section 2 describes first, the ocean model (OGCM) and second the data assimilation scheme used. Assimilation experiments are described in Section 3, with a focus on the assimilated observations data sets. Section 4 describes both the protocol of assimilation experiments and the simulated SSS data used. In Section 5, results are shown and discussed. Section 6 draws some conclusions about what can be expected from SSS assimilation in an ocean forecasting system.

2. Ocean model and assimilation scheme

2.1. The ocean model configuration

In this paper, assimilation experiments have been carried out with a primitive equation model of the North Atlantic basin initially developed for the French CLIPPER project (Tréguier et al., 1999). It is an eddy-permitting model called MNATL which has been used operationally since 2001 at Mercator Ocean. It is also the ocean model used to perform the first MO reanalysis (Greiner et al., 2006).

The numerical code is based on OPA 8.1, a *z*-coordinate primitive equation model developed at LOCEAN (Madec et al., 1998) that uses the hydrostatic approximation and the rigid lid formulation. Vertical mixing of momentum, temperature and salinity is computed according to the turbulent kinetic energy closure model developed by Blanke and Delecluse (1993), with enhanced turbulent viscosity in case of convective situations. The total vorticity term is discretized by an adaptation of the scheme of Arakawa and Lamb (1981) referred to as the energy-enstrophy conserving (EEN) scheme that conserves both total energy and potential enstrophy (Barnier et al., 2006).

The model domain covers the North Atlantic basin from 20°S to 70°N and from 98.5°W to 20°E, with a horizontal resolution of $1/3° \times 1/3°$ cosinus(latitude). The vertical discretization has 42 geopotential levels, with a grid spacing that increases from 12 m at the surface to 200 m below 1500 m depth. The bathymetry is derived from Smith and Sandwell (1997). The model solution is relaxed toward climatology within buffer zones defined off Portugal, in the Norwegian Sea and along the Southern boundary to simulate the supply of Mediterranean Water and the exchange with the Artic and South Atlantic basins respectively.

The thermodynamic variables (temperature and salinity) are initialized from a climatology derived from hydrographic observations and compiled by Reynaud et al. (1998). In this study, no spin-up has been used in order to start assimilation experiments from a non-biased state of the ocean. This method tends consequently to improve the convergence of data assimilation process. The atmospheric forcing fields of heat, freshwater and momentum are derived from the analysis of the ECMWF 6-h forecasts of the 2003 period. In addition, the model surface temperature is relaxed toward daily Real-Time Global SST (RTG-SST) analysis, developed at the Marine Modelling and Analysis Branch (MMAB; http://polar.ncep.noaa.gov/sst/). This kind of relaxing term is used in order to maintain interactivity between the ocean model and the atmosphere (Barnier et al., 1995). The main river outflows are represented by an input of fresh water at the river mouths given by the climatological monthly data base from UNESCO (Vörösmarty et al., 1996).

2.2. The data assimilation scheme

The impact studies presented in this paper have been performed using the new MO operational forecasting system based on the second generation SAM2v1 assimilation scheme (Tranchant et al., 2005). This scheme is being developed in a pre-operational mode for the main MO operational prototypes recently based on the NEMO-OPA code (Madec et al., 1998) which is a free-surface model and for which some significant numerical improvements have been made (Barnier et al., 2006).

The SAM2v1 assimilation scheme is a multivariate assimilation algorithm consisting of a SEEK filter (Brasseur and Verron, 2006). The SEEK filter is a reduced-order Kalman filter introduced by Pham et al. (1998) in the context of mesoscale ocean models and has been designed for a large variety of basin-scale ocean models and validated in many studies (Brasseur et al., 2005; Durand et al., 2002; Durand et al., 2003; Penduff et al., 2002; Testut et al., 2003).

The error statistics of this method are represented in a subspace spanned by generally a small number of dominant 3D error directions. The formulation of the assimilation algorithm relies on a low-rank error covariance matrix, which makes the calculations tractable even with state vectors of very large dimension. Thus, correlations between variables of state vector are defined by this low-rank error covariance matrix. The extrapolation from observed (SLA, *T*, *S*) to non-observed variables (*U*, *V*) is performed along the directions represented by these error modes which connect all dynamical variables and grid points of the numerical domain. Note that a sufficient number of these directions are necessary to obtain a realistic estimation of the error statistics. Unlike the original SEEK filter (Ballabrera-Poy et al., 2001), SAM2v1 does not evolve the error statistics according to the model dynamics. This would require prohibitive costs given the size of the operational system. However, some form of evolutivity of the background error is taken into account by considering different error sub-spaces for the four seasons. An ad-hoc protocol involving the computation of empirical 3D modes obtained from a hindcast simulation (assimilation of SLA and SST data every ten days) performed during the 1993–2001 years has been applied for each season; this approach leads to corrections of the model trajectory that are 3D multivariates and seasonally consistents. In this paper,

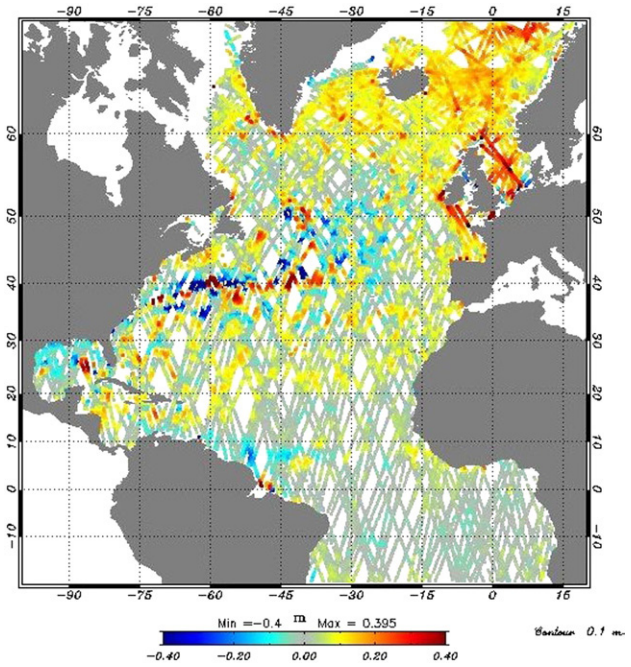

Fig. 1. Example of altimeter data assimilated into the SAM2v1 system for a week. (1–8 January 2003).

four seasonal error covariance matrices based on the first 150 EOFs are used to perform the assimilation experiments.

SAM2v1 uses a diagonal observation error matrix which means that correlated errors are neglected. In order to prevent the data from exerting a spurious influence at remote distances through large-scale signatures in the 3D modes, a simplification of the analysis scheme has been adopted by enforcing to zero the error covariances between distant variables which are believed to be uncorrelated in the real ocean, e.g., Brankart et al. (2003) and Testut et al. (2003). This simplification is implemented in SAM2v1 by assuming that distant observations have negligible influence on the analysis. Moreover, since the SEEK algorithm is a local inverse algorithm, each water column is only influenced by observations in a pre-determinated area called "influence bubble" that varies in space and in time. The size of these influence bubbles have been determined from a previous reanalysis (Greiner, 2006), and have the particularity to be larger in tropical and equatorial regions (zonal direction) than in other regions where mesoscale activity is strongest.

In practice, the SAM2v1 system consists in a sequential scheme based on a 7-day assimilation cycle. The innovation vector (observation minus model counterpart) is calculated during the model integration (the forecast step) using the First Guess at Appropriate Time (FGAT) approximation which corresponds to a misfit between the model and the observation computed at appropriate time. Due to the fast propagation of equatorial waves, the FGAT feature may be particularly important in the tropical oceans (Brasseur, 2006).

3. Assimilation experiments

3.1. The reference simulation

A reference simulation (REF) or control run has been conducted. It consists of a hindcast simulation using the SAM2v1/MNATL system previously detailed, which it is starting in January 2003 from temperature and salinity climatology (Reynaud et al., 1998), and integrated over one year (1st January–31 December 2003) using a 7-day assimilation cycle. The assimilated operational data are described in the following sub-section.

3.2. The operational data set

All the assimilation experiments showed hereafter use the same observation data set which is used in the current MO multi-data and multivariate operational systems. Here, we review briefly the different observation data sets assimilated in our OSSEs.

3.2.1. Altimeter data

The along track sea level anomalies from JASON-1, ERS-2/ENVISAT and GFO satellites are assimilated with the FGAT method. The observation errors covariance matrices are diagonals and equal to 2 cm for JASON, and equal to 3.5 cm for GFO and ERS-2/ENVISAT. About 40,000 data have been selected on the model grid every week. An example is given on

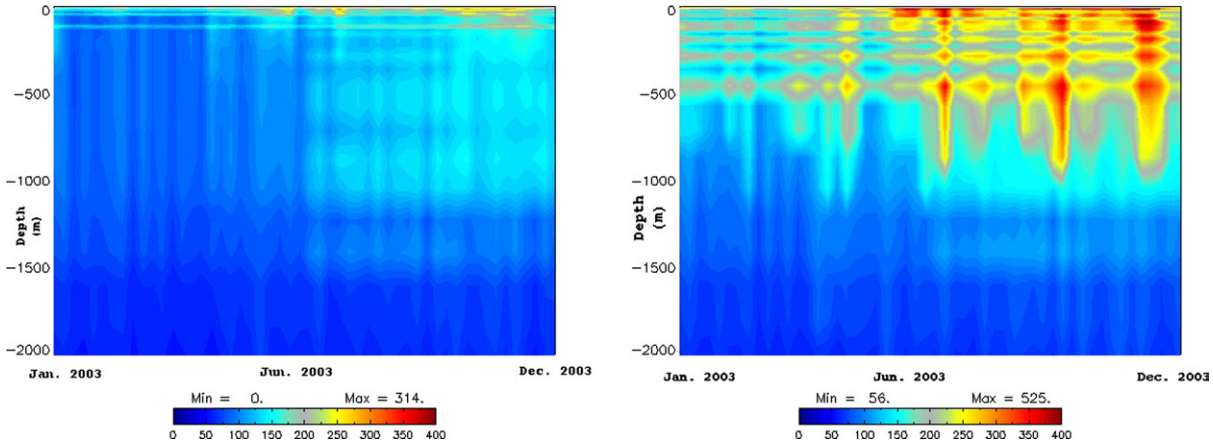

Fig. 2. Number of salinity (left) and temperature (right) profiles between the sea surface and 2000 m depth assimilated during the year 2003 by the SAM2v1 system.

Table 2
Experiments: names and main characteristics of simulated SSS L2 products

Name of the experiment over year 2003	SSS data product characteristics	
	Spatial resolution along tracks every day (km)	Estimated observation error range (RMS in PSU)
SMOS L2	40×40	0.2–2.5
SMOS L2_2	40×40	0.4–5
SMOS L2_0.5	40×40	0.1–1.25
Aquarius L2	100×100	0.1–1.5
SMOS L2+ Aquarius L2	40×40+100×100	0.2–2.5+0.1–1.5

Fig. 1, corresponding to sea level anomalies assimilated during one week of integration from January 1 to January 8, 2003. Every week, three different types of altimeter data lead to a good coverage overall the domain.

3.2.2. MSSH

A pseudo-data of Mean Sea Surface Height (MSSH) coming from a previous work based both on an MO reanalysis and the work of Rio and Hernandez (2004) is used as a reference level for the Sea Surface Height (SSH). An estimate of the MSSH error has been added to the overall altimetric observation error where largest values (~10 cm) are located generally on shelves and along the coast.

3.2.3. In-situ data

Vertical *T*/*S* profiles (down to 2000 m depth in some cases), measured by ARGO floats, XBT/CTDs, moorings or buoys, and provided by the CORIOLIS operational data centre (Brest) are assimilated in SAM2v1 with the FGAT method. About 300 *T*/*S* profiles are selected every week. Fig. 2 represents weekly variations of the number of salinity and temperature profiles over 2003 from surface up to 2000 meter depth. It shows that there are much more temperature profiles than salinity profiles, and they are mainly located in the first 1000 m depth. In addition there is a strong inter-seasonal variation. Observation errors of in-situ data are depth dependent and have been inferred from previous hindcast experiments. Largest values of observation errors are at surface with standard deviations of 0.6 °C and 0.15 PSU for temperature and salinity.

3.2.4. Climatological profiles

Monthly climatology for the temperature and salinity profiles on a 2°×2° grid are assimilated for deep layers at the date of analysis. A limited number of these climatological *T*/*S* profiles are assimilated at the date of analysis from about 500 m depth in tropics and 2000 m depth at higher latitudes to bottom. This assimilation is realized by means of an empirical criterion applied on the error (Greiner et al., 2006) which allows us to keep the meso-scale but also to avoid too large drifts for deep layers.

3.2.5. SST

The sea surface temperature (SST) is the Real Time Global SST analysis product (RTG_SST) from NCEP, available on a 0.5×0.5° grid (Thiébault et al., 2003). This SST is remapped on a 1°×1° grid and is only assimilated at the date of analysis. The associated observation error is spatially constant and fixed to 1.2 °C.

4. OSSEs protocol and simulated SSS data

All data assimilation experiments are similar to the REF experiment (see Section 3.1). They only differ by the additional assimilation of simulated SSS data. The different experiments appear in Table 2 where the characteristics of SSS products described below have been summed up. In this paper, we focus only on data assimilation results, thus no verifications of forecast quality have been done.

4.1. Simulated SSS data: The input field

The initial SSS field simulating the real SSS observed comes from regridded SSS fields generated by the MO PSY2V1 system. This ocean analysis system only assimilates altimeter data contrary to the SAM2V1 scheme previously described which is multivariate and assimilates several data sets (see Section 2.2). Thus, the OSSEs methodology used in this paper avoids the "identical twin" problem since two different ocean forecasting systems are used to generate the simulated

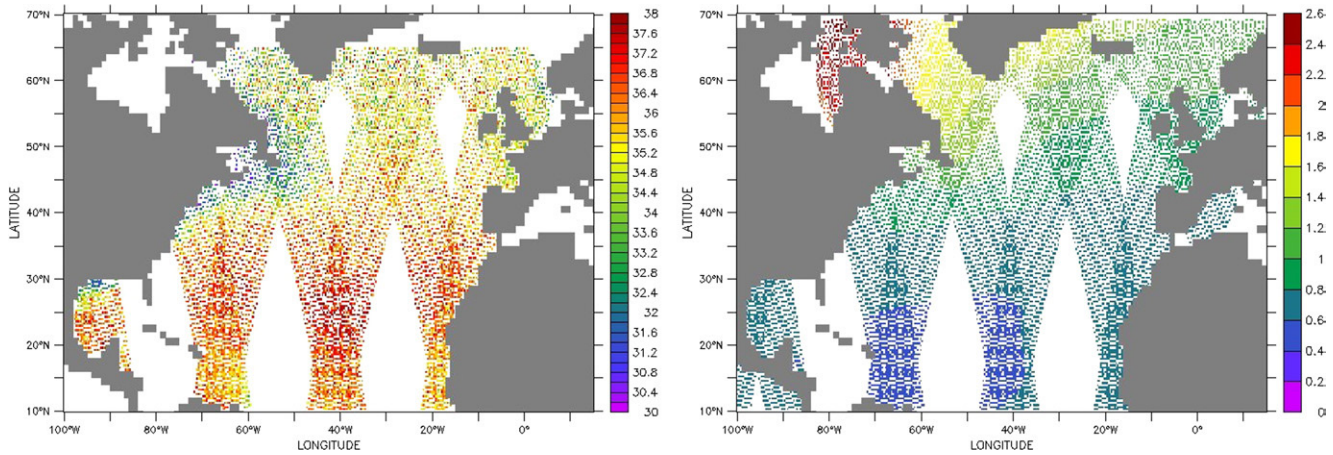

Fig. 3. SMOS pixel location on July 6th 2003 (Level 2): salinity in PSU (left) and the associated RMS errors in PSU (right).

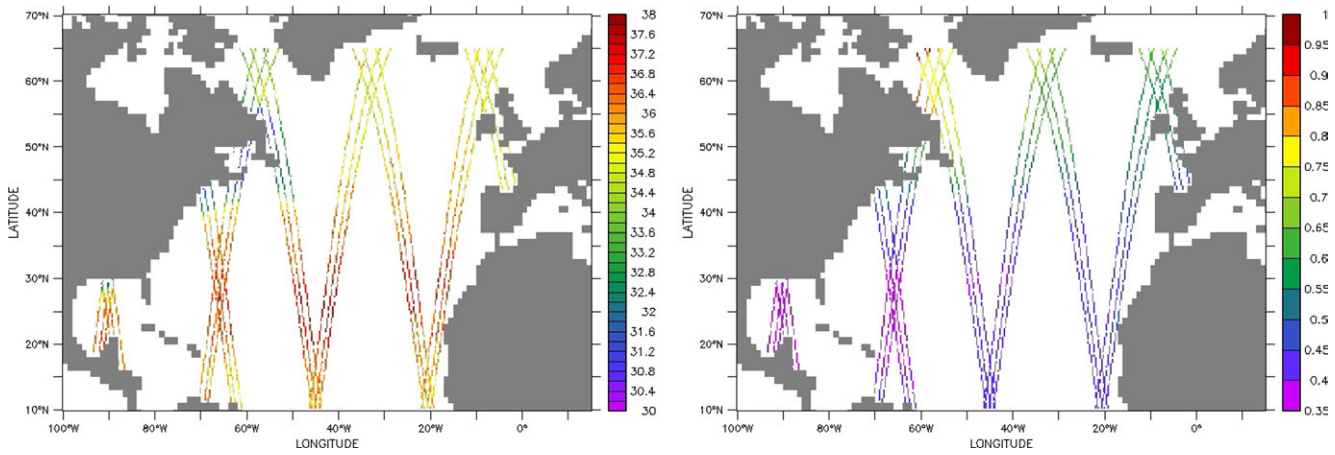

Fig. 4. Aquarius pixel location on July 6th 2003 (Level 2): salinity in PSU (left) and the associated RMS errors in PSU (right).

observations and to test the effectiveness of these observations (see Atlas, 1997). Not only the ocean forecasting systems have different assimilation schemes, but they also differ by their ocean model configurations. The ocean model used in this study (MNATL) is an eddy-permitting model (1/3°) covering the North Atlantic and Tropics (20°S–70°N°) whereas the ocean model used to generate the simulated SSS data is an eddy-resolving model (1/15°) covering North Atlantic and Mediterranean Sea (9°N–70°N).

4.2. Simulated SSS data: Level 2 products

Generally, a Level 2 (or L2) product is defined as a product at the captor pixel resolution (or similar). Most of the simulated SSS products have been processed by Boone et al. (2005). These are the Level 2 products coming from SMOS and Aquarius. In addition to these sets, two new sets of SMOS Level 2 products have been processed by modifying the initial specification of the observation error. SMOS L2 products and their associated errors are based on SSS retrievals from which accuracies are mainly dependant of the brightness temperatures (Tb's) but also of auxiliary parameters such as SST and wind speed, see for example (Boutin et al., 2004; Philipps et al., 2005).

SMOS L2 product are generated from daily SSS fields over 2003 from MO PSY2-V1 (9°N–70°N) resampled at 1/3° (roughly equivalent to the 40 km^2 SMOS mean pixel area) fields. It is then sub-sampled on the pixel daily location corresponding to the effective satellite tracks. A Gaussian noise associated to the prior specification of the future SMOS satellite is then added to this field. This error varies in space and time. It defines the initial specifications of the observation errors. An example of simulated daily SMOS SSS measurements along tracks and their associated observation errors for July 6, 2003 is given on Fig. 3.

For a better understanding of the impact of SSS observation errors, two other modified data sets from the initial Level 2 SSS data coming from Boone et al. (2005) have been generated (L2_2 and L2_0.5). Data locations along simulated SMOS satellite tracks have been preserved, only values and associated errors have changed. The data values have been regenerated by multiplying both the initial Gaussian noise and the associated RMS of observation errors by 2 and by 0.5.

Knowing the orbital and instrument characteristics, the same protocol as SMOS L2 data has been used for the generation of Aquarius L2 data. A noise estimated from Boone et al. (2005) is added to the daily MO PSY2V1 SSS over 2003. The spatial resolution is about 100 km × 100 km along simulated Aquarius satellite tracks. Fig. 4 represents simulated daily Aquarius SSS measurements along tracks and their associated observation errors for July 6, 2003. Compared to the daily coverage of SMOS SSS data (Fig. 3), the daily coverage of Aquarius SSS data is lesser (Fig. 4). Nevertheless, the observation errors of Aquarius are approximately two times weaker than those of SMOS.

Actually, experiments can be distinguished by: (i) the spatial and time resolution of simulated SSS data, and (ii) the estimated observation errors of simulated SSS data. All experiments are listed in Table 2.

5. Results

Mean and variance of the difference between experiments and "truth" have been calculated on the domain corresponding to geographic locations of simulated SSS data, i.e., the North Atlantic PSY2v1 domain (9°N to 70°N). This difference is a measure of the analysis skill when simulated SSS data are assimilated. It shows the ability of the assimilation system in handling various sources of errors (data and model). The "truth"

Table 3
RMS of difference between experiments and "truth" overall the domain (year 2003)

Name of experiment	REF	SMOS L2_2	SMOS L2	SMOS L2_0.5	Aquarius L2	SMOS L2 + Aquarius L2
RMS (PSU) of the difference between experiment and "truth" overall the domain (year 2003)	0.4859	0.3945	0.3104	0.2847	0.4353	0.3077

is the original SSS located on the SMOS L2 products, i.e., the original SSS coming from the North Atlantic and Mediterranean high resolution MO prototype named PSY2V1 resampled at 1/3°, see Section 4. We only calculated statistics relative to the "truth" and not to independent data. Indeed, the main drawback of this study is that the "truth" is too far from a realistic SSS field. It is thus difficult to compare with independent data or to compare with others variables of interest at various depths.

OSSEs results are summarized in Table 3 where RMS of difference (PSU) between all OSSE experiments and "truth" averaged overall the domain are reported.

5.1. Impact of the observation errors

Because the assimilation impact of one dataset is related to the observation error ratio between each dataset, it is interesting to compare various observation errors levels. This sensitivity to the observation error level is very important in a system assimilating combined data. The annual mean and variance of the difference between three experiments (SMOS L2, SMOS L2_2 and SMOS L2_0.5) and the "truth" averaged over the year 2003 are showed in Fig. 5. In general, the smaller the observation error is, the weaker are the mean and variance of the difference. Some regions can be distinguished according to the skill of the assimilation system in reducing the difference when simulated SSS products are assimilated (e.g., at the river mouths). Differences are generally highest: (i) in high latitudes where observation errors are highest, (ii) in the Gulf Stream where variability is high, (iii) near the coast where the assimilation system presents some limitations to assimilate observations with too important errors.

For SMOS L2_0.5 and SMOS L2, important biases have been removed. In some regions, the variance of difference has

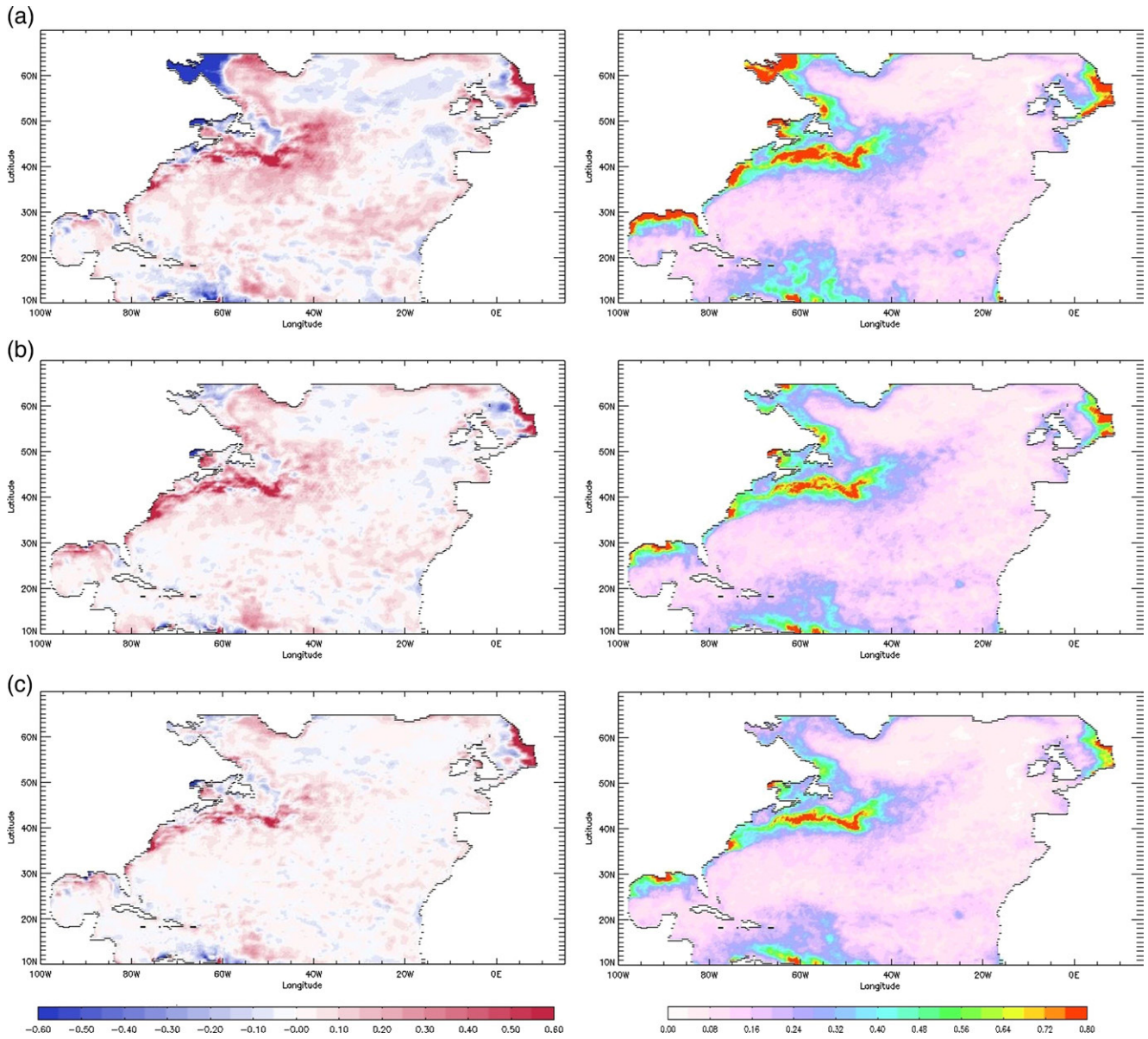

Fig. 5. Mean (left) and variance (right) of difference between three different estimates: SMOS L2_2 (a), SMOS L2 (b), SMOS L2_0.5 (c) and "truth" averaged over the year 2003.

been divided by 2 when SSS SMOS L2 products (data and associated errors) prescribed by Boone et al. (2005) are assimilated, thus reducing the RMS of the mean difference from around 0.5 to 0.3 PSU, see Table 3. On the one hand, even if this impact is weaker for SMOS L2_2, Fig. 6 shows that excepted for REF, the time evolution of the mean difference is quite equivalent for all experiments. On the other hand, the time evolution of the variance for SMOS L2_2 is similar to REF during the first three months. It shows that it takes three months until the SSS assimilation exerts a significant influence (after three months, the time evolution of variance is equivalent to SMOS L2_0.5 and SMOS L2).

Small scales are certainly more constrained for SMOS L2 and SMOS L2_0.5 which use lower observation errors. The level of SSS observation error in the SMOS L2_2 appears too weak in comparison to the other data constraints. Here, one can introduce the concept of threshold since a minimum level of observation errors (as specified into the SMOS L2 experiment) is necessary to obtain a significant impact in a system close to the current multivariate and multi-data MO data assimilation system. Obviously, some future improvements both in term of additional data sets or in term of better estimation of observation error could modify this threshold. In addition, to date, only random errors have been included in the simulated observations and no systematic large-scale errors have been taken into account. This weakness in the estimation of the simulated error may also mask or reduce the impact of simulated observations from other observing systems.

5.2. Impact of assimilating different observing systems

The results come from the comparisons of various assimilation experiments using two different data types (SMOS L2, Aquarius L2) and combinations of these two data types (SMOS L2 + Aquarius L2).

The difference (mean and variance) of four experiments (REF, SMOS L2, Aquarius L2 and Aquarius + SMOS L2) are showed in Fig. 7. The time evolution of mean and variance of differences during 2003 are showed in Fig. 8. At first, we can see that the difference between REF and the "truth" is not spatially homogeneous. In particular, important patterns appear in three types of regions: (1) turbulent regions characterised by meso-scale activity (Gulf Stream); (2) coastal regions where river runoff play a significant role (Mississippi delta, Gulf of Saint-Laurent, …); (3) and more specific regions as such the North Sea where oceanic solutions provided by our system are relatively unrealistic.

In comparison to the REF experiment, the SMOS L2 simulation (Fig. 7c) presents some significant and very important decreasing of the difference to the "truth" in regions of interest. Thus, the effects are strong in regions of river runoff and in the Gulf Stream current. However, as expected, the important pattern in the North Sea is not sufficiently reduced, which is essentially due to the weakness of the ocean model to represent significant physical processes in this coastal region.

The Aquarius L2 differences are lesser than those found with SMOS L2 experiments. The Aquarius L2 simulation (Fig. 7b) is relatively better than the REF experiment which means that the SSS constraint coming from the simulated Aquarius observation system acts favourably on our data assimilation system. However, this impact seems to be weak in comparison to the SMOS L2 simulation. Several explanations can be proposed for the relative inefficiency of the Aquarius L2 simulation in comparison to the SMOS L2 simulation. Each of them contributes to explain results obtained from the Aquarius L2 simulation. First, the daily data coverage is very different between these two products. The SMOS L2 space and time coverage is approximately twice as large as the one from Aquarius L2. The SSS SMOS L2 Products are thus associated to a stronger constraint in the assimilation step than the Aquarius L2 Products. Moreover, it is interesting to note that the decorrelation scales (in days) in a 1/3° reanalysis over 11 years (Greiner, 2006) shown in Fig. 9 is generally less than 4 days. It is representative of the ocean–atmosphere exchange processes

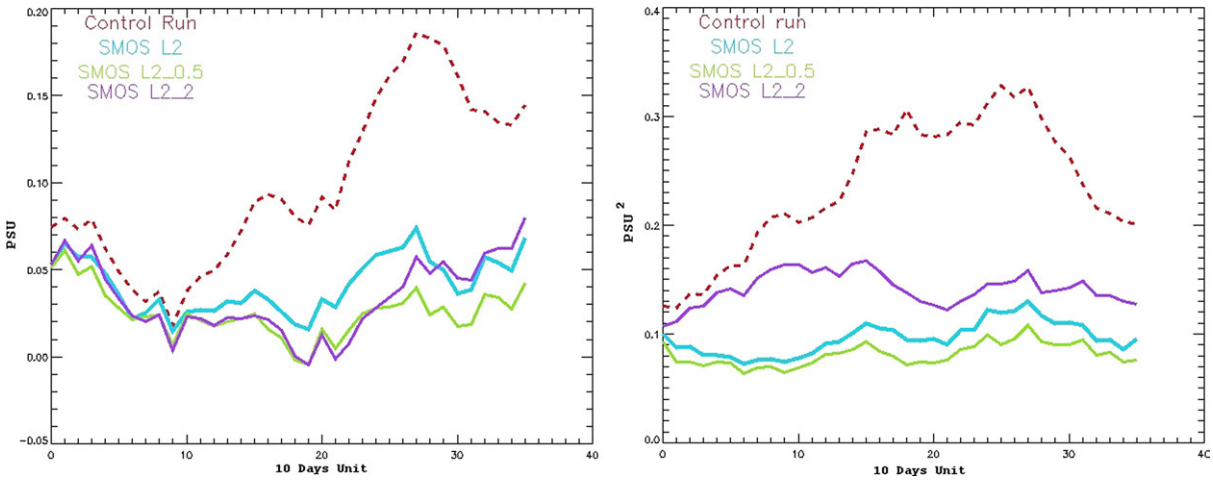

Fig. 6. Spatial average of the mean in PSU (left) and variance in PSU^2 (right) of difference between three different estimates: control run or REF (red dashed line), SMOS L2 (blue solid line), SMOS L2_0.5 (green solid line), SMOS L2_2 (purple solid line) and "truth" every ten days during the year 2003 for the overall domain.

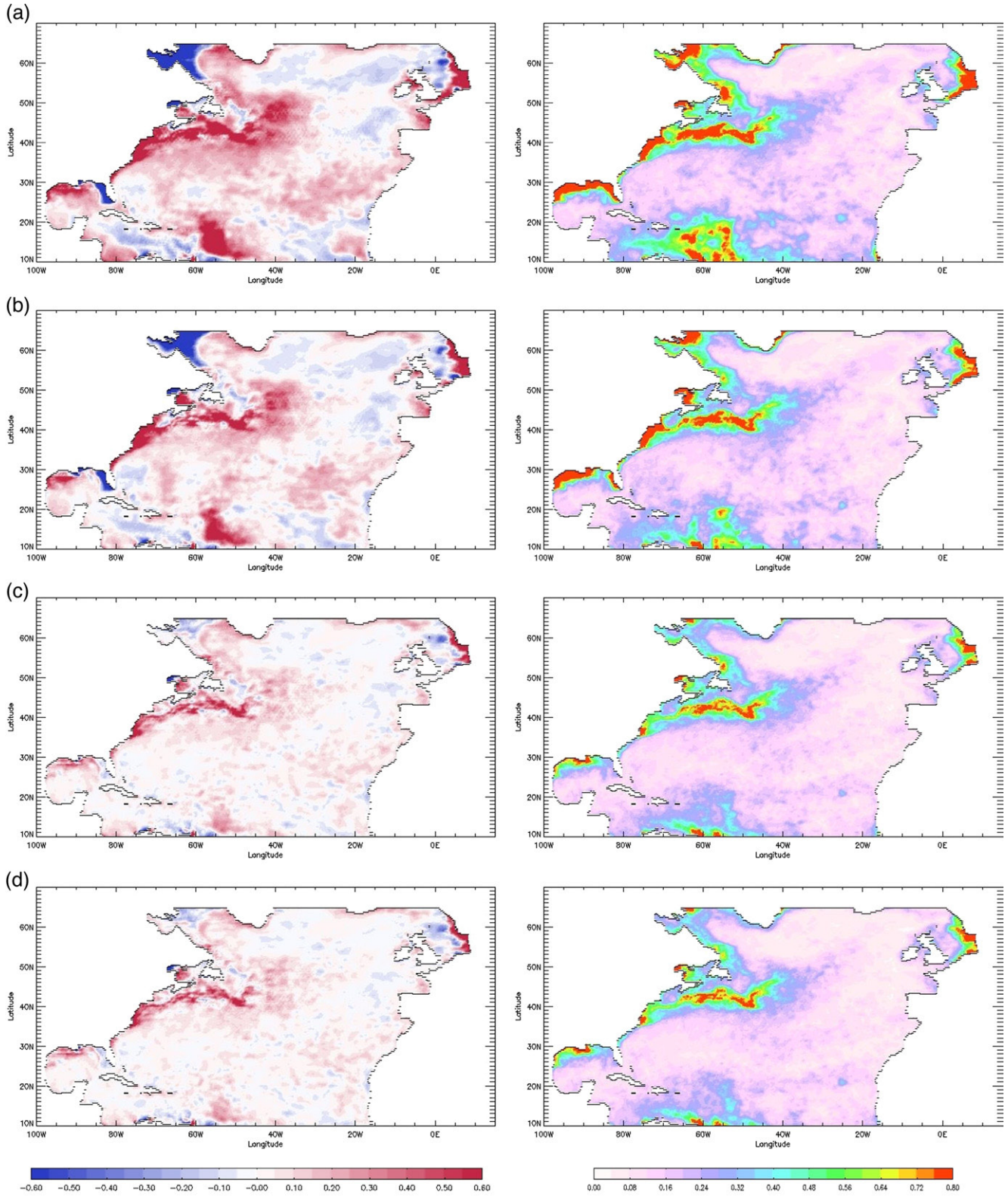

Fig. 7. Mean (left) in PSU and variance (right) in PSU^2 of difference between three different estimates: Reference (a), Aquarius L2 (b), SMOS L2 (c) and Aquarius + SMOS L2 (d) and "truth" averaged over the year 2003.

that take place in the North Atlantic. But, since each ocean grid point is observed by Aquarius measurements every 7 days and by SMOS measurements every 3 days, only SMOS L2 data are able to constraint an eddy-permitting model (spatial resolution less than or equal to 1/3°). Second, the error associated to Aquarius L2 Products is smaller than that of SMOS L2 Products. Typically at 40°N, SMOS L2 error is about 1 PSU (RMS) whereas Aquarius L2 error about 0.5 PSU (RMS).

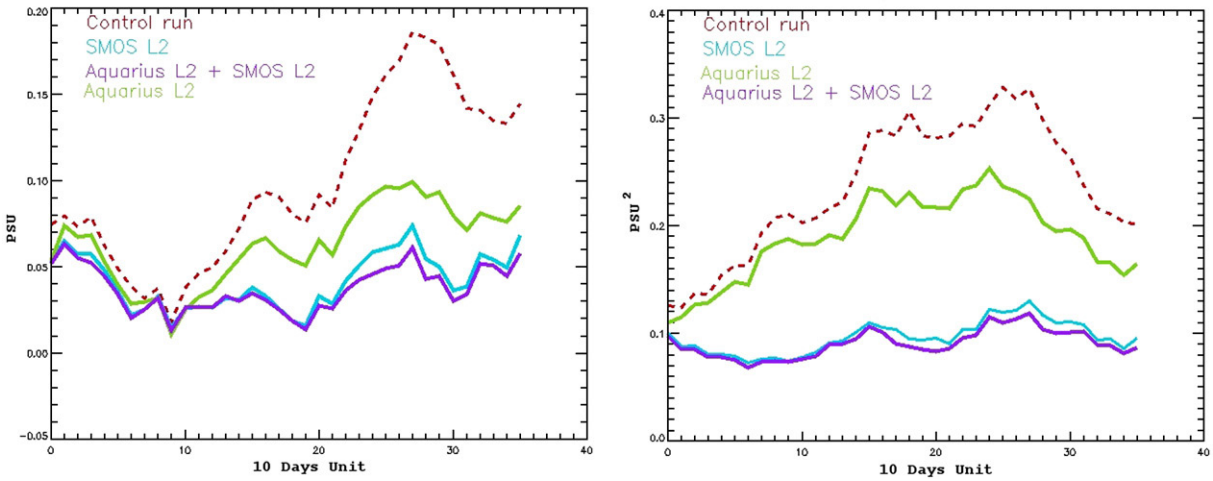

Fig. 8. Spatial average of the mean in PSU (left) and variance in PSU^2 (right) of difference between three different estimates control run or REF (red dashed line), SMOS L2 (blue solid line), Aquarius L2 (green solid line), SMOS L2 + Aquarius L2 (purple solid line) and "truth" every ten days during the year 2003 for the overall domain.

Nevertheless, remapped onto the Aquarius grid (100 × 100 km), and using a non-correlated errors assumption, the equivalent SMOS L2 observation error becomes smaller, i.e., 0.4 PSU (RMS) on the Aquarius grid (100 km × 100 km). At last, the spatial resolution of Aquarius is also a potential explanation of the difference. Indeed, the Aquarius Level 2 data (100 km × 100 km) are not able to constrain smaller scales.

It seems relatively difficult to really distinguish the impact of each of these reasons in the difference between the SMOS L2 and Aquarius L2 simulations.

As expected, the impact of the assimilation experiment combining the two simulated SMOS L2 and Aquarius L2 Products is weak compared to the SMOS L2 simulation (Fig. 8), and it is slightly marked at the end of the simulation by improving statistical results.

6. Conclusions

In the context of the SMOS and Aquarius missions, final products will be strongly constrained by the complexity of SSS

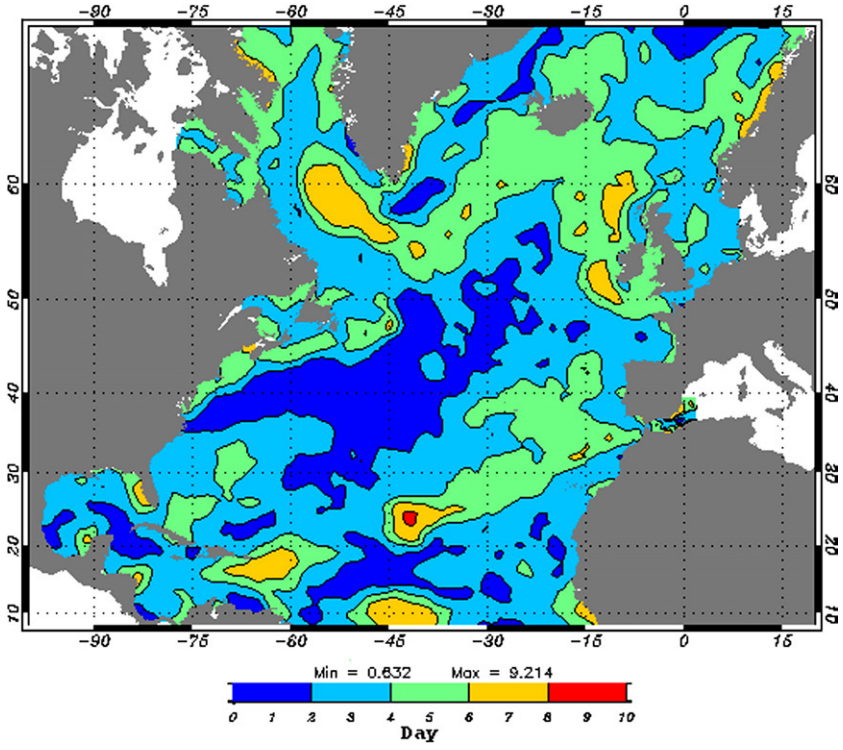

Fig. 9. Temporal decorrelation scales (day unit) from a re-analysis at 1/3°(10°N–70°N) over 11 years (1992–2002) calculated from annual time series. Limit of time correlation is fixed at 0.4.

retrieval. In connexion with that, Boutin et al. (2004) showed the importance to have accurate auxiliary data such as SST. In a recent study, Maes et al. (2006) showed that correlations exist between warm SSTs and low salinities in the western Pacific warm pool. In the same way, results of Wang and Chao (2004) on the SSS variability confirmed the designing strategy of the upcoming SSS satellite missions. An important question is then: "what is the best strategy to optimally use the future SMOS and Aquarius data in the context of ocean prediction systems, from the perspective of monitoring the mesoscale ocean circulation?"

For this reason, OSSEs performed with the MO assimilation system SAM2v1 tried to estimate the best level and accuracy of SSS product which will have a sufficient positive impact on the MO forecasting system. On one hand, these OSSEs have been performed with two different satellites (SMOS and Aquarius) products and different observation errors coming from Boone et al. (2005). On the other hand, as mentioned by Atlas (1997), these results are only valid for instruments meeting expected accuracies and coverages that were simulated.

From our results, several conclusions can be highlighted.

The use of the synthetic SMOS L2 product gives satisfactory improvement in the model results, since it provides a measurable impact of the quality of ocean analyses from operational systems. The SSS observation error variance as specified by Boone et al. (2005) and particularly its ratio with regard to the error of the other data sets assimilated seems appropriate.

The impact of the Aquarius L2 Products is weak compared to the SMOS L2 Products. The combination of the two L2 Products had thus a small effect on final results. Further studies are necessary to better understand this feature of the Aquarius L2 Products. In particular, it is interesting to distinguish the main reasons of this weakness between several possible explanations: (i) the spatial coverage which is less than the SMOS L2 Products (ii) the potential underestimation of the specified SMOS L2 observation errors, (iii) the potential overestimation of the Aquarius L2 observation errors, (iv) the magnitude of the observation error, (v) and the difference of resolution between model (roughly 40×40 km) and data (100×100 km). Furthermore, a combined multidata (SMOS and Aquarius) Product on the same time and space scales as those of the initial SMOS L2 Products could be a better compromise for our oceanic solution. Wang and Chao (2004) note that the ability to estimate SSS variability shorter than 30 days will be continuously improved in the anticipation of assimilating the SSS observation.

These conclusions have to be counterbalanced by the fact that real-time data used operationally (SLA, SST and in-situ) have been assimilated into the assimilation system. Indeed, the assimilated simulated SSS data comes from SSS field relatively far from the other assimilated data. It is possible, thus, that this data incoherency leads to spurious effects. Generally, it is difficult to discriminate effects in favour of one parameter due to interactions between the parameters (observation errors, observation operator, error covariances…). For example, due to the fact that the assimilation system does not correct any fluxes, in particular the $E-P$ fluxes, it leads to underestimate information coming from SSS.

The next step would be to introduce the multi-mission concept, i.e., assimilating SMOS and Aquarius combined products on the same time and space scales as the SMOS L2 products which seem more appropriate for our system. The extension of SSS assimilation in a global model (low and high resolution) in order to apprehend important physical processes in Pacific and Tropical regions (Delcroix et al., 2005; Maes et al., 2006) is essential.

Obviously, the data assimilation scheme takes also an important part in our experiments. It seems necessary to improve it by a better control of air–sea fluxes which could reduce the model background error and then enhance the interest to have more precise observations. Stammer et al. (2004) have proposed a new estimation of air–sea fluxes through an iterative method based on the "adjoint" method. Note also that the SSS variability on different time scales and more generally the existence of different time scales in the ocean is a property that can be exploited by developing advanced observation operators or improved background error covariance models.

Acknowledgements

This work was partly supported by the European Space Agency (ESA). We express our gratitude to Christine Boone and Estelle Obligis for having made the simulated SSS data available. Fruitful discussions with Eric Greiner about the MERA11 reanalysis were particularly appreciated.

References

Arakawa, & Lamb (1981). A potential enstrophy and energy conserving scheme for the shallow water equations. *Monthly Weather Review*, *vol. 109*, 18−36.

Atlas, R. (1997). Atmospheric observations and experiments to asses their usefulness in data assimilation. *Journal of Metrology Society of Japan*, *vol 75*(No, 1B), 111−130.

Ballabrera-Poy, J., Brasseur, P., & Verron, J. (2001). Dynamical evolution of the error statistics with the SEEK filter to assimilate altimetric data in eddy-resolving ocean models. *Q.J.R. Metals Society*, *127*, 233−253.

Barnier, B., Siefrift, L., & Marchesiello, P. (1995). Thermal forcing for a global ocean circulation model using a three-year climatology of ECMWF analyses. *Journal of Marine Systems*, *6*, 363−380.

Barnier, B., Madec, G., Penduff, T., Molines, J. M., Tréguier, A. M., Le Sommer, J., et al. (2006, March). Impact of partial steps and momentum advection schemes in a global ocean circulation model at eddy-permitting resolution.*Ocean Dynamics* (doi 10.10007/s10236-006-0082-1).

Blanke, B., & Delecluse, P. (1993). Variability of the tropical Atlantic Ocean simulated by a general circulation model with two different mixed-layer physics. *Journal of Physical Oceanography*, *23*, 1363−1388.

Boone, C., Larnicol, G. and Obligis, E. (2005), WP2000: Characteristics of SMOS/AQUARIUS level-3 product, July 2005, CLS-DOS-NT-05-116.

Boutin, J., Waldteufel, P., Martin, N., Caudal, G., & Dinnat, E. (2004). Surface salinity retrieved from SMOS measurements over the global ocean: Imprecisions due to sea surface roughness and temperature uncertainties. *Journal of Atmospheric and Oceanic Technology*, *21*, 1432−1447.

Brankart, J. -M., Testut, C. -E., Brasseur, P., & Verron, J. (2003). Implementation of a multivariate data assimilation scheme for isopycnic coordinate ocean models: Application to a 1993–96 hindcast of the North Atlantic Ocean circulation. *Journal of Geophysical Research*, *108*, 3074. doi:10.1029/2001JC001198

Brasseur, P. (2006). Ocean data assimilation using sequential methods based on the Kalman Filter. In J. Verron & E. Chassignet (Eds.), *GODAE, an Integrated View of Oceanography: Ocean Weather Forecasting in the 21st Century* (pp. 577). Kluwer: Academic Press.

Brasseur, P., & Verron, J. (2006, August). The SEEK filter method for data assimilation in oceanography: A synthesis. *Ocean Dynamics*. doi:10.1007/s10236-006-0080-3

Brasseur, P., Bahurel, P., Bertino, L., Birol, F., Brankart, J. M., Ferry, N., et al. (2005). Data assimilation in operational ocean forecasting systems: The MERCATOR and MERSEA developments.*Q.J.R. Metals Society*, *613*(C), 3561−3582 (22).

Cooper, N. S. (1988). The effect of salinity on Tropical Ocean Models. *Journal of Physical Oceanography*, *18*, 697−707.

Delcroix, T., McPhaden, M. J., Dessier, A., & Gouriou, Y. (2005). Time and space scales for sea surface salinity in tropical oceans. *Deep-Sea Research. Part 1*, *52*, 787−813.

Dessier, A., & Donguy, J. -R. (1994). The sea–surface salinity in the tropical Atlantic between 10°S and 30°N, seasonal and interannual variations (1977–1989). *Deep-Sea Research I*, *41*, 81−100.

Durand, F., Gourdeau, L., Delcroix, T., & Verron, J. (2002). Assimilation of Sea surface Salinity in a Tropical OGCM: A twin experiment approach. *Journal of Geophysical Research*, *107*(C12), 8010. doi:10.1029/2001JC000849

Durand, F., Gourdeau, L., Delcroix, T., & Verron, J. (2003). Can we improve the representation of modeled ocean mixed layer by assimilating surface-only satellite-derived data? A case study for the tropical Pacific during the 1997–1998 El Niño. *Journal of Geophysical Research*, *108*(C6), 3200. doi:10.1029/2002JC001603

Ferry, N., & Reverdin, G. (2004). Sea surface salinity interannual variability in the western tropical Atlantic: An ocean general circulation model study. *Journal of Geophysical Research*, *109*(C5). doi:10.1029/2003JC002122 (issn: 0148-0227).

Font, J., Kerr, Y., & Berger, M. (2000). Measuring ocean salinity from space. *Backscatter*, *11*, 17−19.

Godfrey, J. S., & Lindstrom, E. J. (1989). The heat budget of the equatorial western Pacific surface mixed layer. *Journal of Geophysical Research*, *94*, 8007−8017.

Greiner, E. (2006). The Mercator 1992–2002 PSY1v2 ocean reanalysis for tropical and North Atlantic, (2006). *Proceeding of 15 years of progress in radar altimetry symposium* : Venice (Italy) (13–18 March 2006).

Greiner, E., Benkiran, M., Blayo, E., and Dibarboure, G. (2006), MERA11, General Scientific Paper 1992–2002 PSY1v2 reanalysis, September 2006, MOO-MR-431-37-MER.

Kamenkovich, I. V., & Sarachik, E. (2004). On reducing errors in temperature and salinity in an ocean model forced by restoring boundary conditions. *Journal of Physical Oceanography*, *34*, 1856−1869.

Lagerloef, G., & Delcroix, T. (2001). Sea surface salinity: A regional case study for the tropical Pacific. *Observing the Ocean in the 21st centuryAust. Bur. of Meteorolog*. (pp. 137−148) Victoria: Melbourne.

Lagerloef, G. S. E. (2002). Introduction to the special section: The role of surface salinity on upper ocean dynamics, air–sea interaction and climate. *Journal of Geophysical Research*, *Vol. 107*(N0.C12), 8000 (doi 10,1029/2002JC001669).

Madec, G., Delecluse, P., Imbart, M., & Levy, C. (1998). *OPA 8.1 general circulation model reference manual. Notes de l'IPSL no. 11.*Parie: Université P. et M. Curie (91 pp).

Maes, C., Kentaro, K., Delcroix, T., Kessler, W. S., McPhaden, M., & Roemmich, D. (2006). Observed correlation of surface salinity, temperature and barrier layer at the eastern edge of the western Pacific warm pool. *Geophysical Research Letters*, *33*, L06601. doi:10.1029/2005GL024772

Masson, S., & Delecluse, P. (2001). Influence of the Amazon river runoff on the tropical Atlantic. *Physics and Chemistry of the Earth*, *26*, 137−142.

Murtuggude, R., & Busalacchi, A. J. (1998). Salinity effects in a tropical ocean model. *Journal of Geophysical Research*, *103*, 3283−3300.

Penduff, Th., Brasseur, P., Testut, C. -E., Barnier, B., & Verron, J. (2002). Assimilation of sea–surface temperature and altimetric data in the South Atlantic Ocean: Impact on basin-scale properties. *Journal of Marine Research*, *60*, 805−833.

Pham, D. T., Verron, J., & Roubaud, M. C. (1998). Singular evolutive extended Kalman Filter with EOF initialization for data assimilation in oceanography. *Journal of Marine Systems*, *16*(3-4), 323−340.

Philipps S, Boone C. and Obligis E. (2005), "The role of averaging for improving sea surface salinity retrieval from the Soil Moisture and Surface Salinity (SMOS) satellite and impact of auxiliary data", accepted to appear in Journal of Atmospheric and Oceanic Technology.

Reynaud, T., Legrand, P., Mercier, H., & Barnier, B. (1998). A new analysis of hydrographic data in the Atlantic and its application to an inverse modelling study. *International WOCE Newsletter*, 32.

Rio, M. -H., & Hernandez, F. (2004). A mean dynamic topography computed over the world ocean from altimetry, in situ measurements, and a geoid model. *Journal of Geophysical Research*, *109*, C12032. doi:10.1029/2003JC002226

Roemmich, D., Morris, M., Young, W., & Donguy, J. R. (1994). Fresh equatorial jets. *Journal of Physical Oceanography*, *24*, 540−558.

Sen, A., Kim, Y., Caruso, D., Lagerloef, G. S. E., Colomb, R., Le Vine, D. M., et al. (2006). *Aquarius/SAC-D mission overview, SPIE 13th International Symposium on Remote Sensing, 11–16 September 2006.* Sweden: Stockholm.

Smith, W. H. F., & Sandwell, D. T. (1997). Global sea floor topography from satellite altimetry and ship depth soundings. *Science*, *277*, 1956−1962.

Stammer, D., Ueyoshi, K., Köhl, A., Large, W. L., Josey, S. A., & Wunsch, C. (2004). Estimating air–sea fluxes of heat, freshwater, and momentum through global ocean data assimilation. *Journal of Geophysical Research*, *109*, C05023. doi:10.1029/2003JC002082

Testut, C. E., Brasseur, P., Brankart, J. M., & Verron, J. (2003). Assimilation of sea surface temperature and altimetric observations during 1992–1993 into an eddy-permitting primitive equation model of the North Atlantic Ocean. *Journal of Marine Systems*, *40-41*, 291−316 (april 2003).

Thiébault, J., Rogers, E., Wang, W., & Katz, B. (2003). A new high-resolution blended real-time global sea surface temperature analysis. *Bulletin of the American Meteorological Society*, *84*, 645−656.

Tranchant, B., Testut, C. E., Ferry, N., Birol, F., & Brasseur, P. (June 2005). SAM2: The second generation of Mercator assimilation system. *Proceeding of the 4th international Conference on EUROGOOS.* (pp. 650−655) (Brest).

Tréguier, A. -M., Reynaud, T., Pichevin, T., Barnier, B., Molines, J. -M., et al. (1999). The CLIPPER Project: High resolution modelling of the Atlantic. *International WOCE Newsletter*, *Nr. 36*, S. 3−S. 5.

Vialard, J., Delecluse, P., & Menkes, C. (2002). A modelling study of salinity variability and its effects in the tropical Pacific Ocean during the 1993–1999 period. *Journal of Geophysical Research*, *107*(C12), 8005. doi:10.1029/2003JC000758

Vörösmarty, C. J., Fekete, B., & Tucker, B. A. (1996). *River Discharge Database, Version 1.0 (RivDIS v1.0), Volumes 0 through 6. A contribution to IHP-V Theme 1.* Paris: Technical Documents in Hydrology Series. UNESCO.

Wang, X., & Chao, Y. (2004). Simulated Sea Surface variability in the tropical Pacific. *Geophysical Research Letters*, *31*, L02302. doi:10.1029/2003GL018146

Yu, L., Weller, R. A., & Sun, B. (2004). Improving Latent and Sensible Heat Flux Estimates for the Atlantic Ocean (1988–99) by a Synthesis Approach. *Journal of Geophysical Research*. doi:10.1175/1520-0442(2004)